Intelligent GNSS Positioning using 3D Mapping and Context Detection for Better Accuracy in Dense Urban Environments

Paul D Groves, Mounir Adjrad, Han Gao and Claire Ellul
University College London

BIOGRAPHY

Dr Paul Groves is a Senior Lecturer (associate professor) at UCL, where he leads a program of research into robust positioning and navigation within the Space Geodesy and Navigation Laboratory (SGNL). He joined in 2009, after 12 years of navigation systems research at DERA and QinetiQ. He is interested in all aspects of navigation and positioning, including improving GNSS performance under challenging reception conditions, advanced multisensor integrated navigation, and novel positioning techniques. He is an author of more than 80 technical publications, including the book *Principles of GNSS, Inertial and Multi-Sensor Integrated Navigation Systems*, now in its second edition. He holds a bachelor's degree and doctorate in physics. (p.groves@ucl.ac.uk)

<DELETED>

Han Gao is a PhD student at University College London (UCL) in the Engineering Faculty's Space Geodesy and Navigation Laboratory (SGNL). He received a Bachelor's degree in Aerospace Engineering from Shanghai Jiao Tong University (SJTU) in 2014. He is interested in multi-sensor contextual navigation and positioning techniques. (han.gao.14@ucl.ac.uk)

Dr Claire Ellul is a Reader (associate professor) at UCL, specializing in Three-Dimensional Geographical Information Science (3D GIS), with a particular interest in 3D usability – including rendering and analytical (topological) performance of large 3D city models on mobile devices and real-world applications of 3D GIS. Prior to becoming an academic, she spent 10 years as a GIS consultant and systems integration specialist.

ABSTRACT

Conventional GNSS positioning in dense urban areas can exhibit errors of tens of meters due to blockage and reflection of signals by the surrounding buildings. Here, we discuss the intelligent urban positioning (IUP) 3D-mapping-aided (3DMA) GNSS concept. This combines conventional ranging-based GNSS positioning enhanced by 3D mapping with the GNSS shadow-matching technique. Shadow matching determines position by comparing the measured signal availability with that predicted over a grid of candidate positions using 3D mapping. Thus, IUP uses both pseudo-range and signal-to-noise measurements to determine position. All algorithms incorporate terrain-height aiding and use measurements from a single epoch in time.

<DELETED>

Navigation and positioning is inherently dependent on the context, which comprises both the operating environment and the behaviour of the host vehicle or user. No single technique is capable of providing reliable and accurate positioning in all contexts. In order to operate reliably across different contexts, a multi-sensor navigation system is required to detect its operating context and reconfigure the techniques accordingly. Specifically, 3DMA GNSS should be selected when the user is in a dense urban environment, not indoors or in an open environment. Algorithms for detecting indoor and outdoor context using GNSS measurements and a hidden Markov model are described and demonstrated.

1. INTRODUCTION

This work was first presented at ION GNSS+ 2016 **Error! Reference source not found.**[2]. Further details of <DELETED> context determination are presented in <DELETED> [2], <DELETED>

The positioning performance of global navigation satellite systems (GNSS) in dense urban areas is poor because buildings block, reflect and diffract the signals. If the real-time position accuracy using low-cost equipment could be improved to 5m or better, a host of potential applications would benefit. These include situation awareness of emergency, security and military personnel and vehicles; emergency caller location; mobile mapping; tracking vulnerable people and valuable assets; intelligent mobility; location-based services; location-based charging; augmented reality; and enforcement of curfews, restraining orders and other court orders. A further accuracy

improvement to around 2m would also enable navigation for the visually impaired; lane-level road positioning for intelligent transportation systems; aerial surveillance for law enforcement, emergency management, building management and newsgathering; and advanced rail signaling.

Buildings and other obstacles degrade GNSS positioning in three ways. Firstly, where signals are completely blocked, they are simply unavailable for positioning, degrading the signal geometry. Secondly, where the direct signal is blocked (or severely attenuated), but the signal is received via a (much stronger) reflected path, this is known as non-line-of-sight (NLOS) reception. NLOS signals exhibit positive ranging errors corresponding to the path delay (the difference between the reflected and direct paths). These are typically a few tens of meters in dense urban areas, but can be much larger if a signal is reflected by a distant building. Thirdly, where both direct line-of-sight (LOS) and reflected signals are received, multipath interference occurs. This can lead to both positive and negative ranging errors, the magnitude of which depends on the signal and receiver designs. NLOS reception and multipath interference are often grouped together and referred to simply as "multipath". However, to do so is highly misleading as the two phenomena have different characteristics and can require different mitigation techniques [3].

There are many different approaches to multipath and NLOS mitigation [4]. A good GNSS antenna is more sensitive to right-hand circularly polarized (RHCP) signals than to left-hand circularly polarized (LHCP) signals. As direct LOS signals are RHCP while most reflected signals are LHCP or mixed polarization, this reduces multipath errors by attenuating the reflected signal components with respect to the direct. Furthermore, NLOS reception can usually be detected from the signal to noise ratio (SNR) measurements, enabling NLOS signals to be eliminated from the position calculation. However, cheaper antennas offer less polarization discrimination and smartphone antennas none at all.

Much of the literature on multipath mitigation is dominated by receiver-based signal-processing techniques [5]. However, because they work by separating out the direct and reflected signals within the receiver, they can only be used to mitigate multipath; they have no effect on NLOS reception at all. Consistency checking selects the most consistent subset of the signals received to compute a position solution from. This is based on the principle that measurements from "clean" direct LOS signals produce a more consistent navigation solution than those from NLOS and severely multipath-contaminated signals. In dense urban areas, a subset comparison approach is more robust that conventional sequential testing [6].

Over the past six years, there has been a lot of interest in 3D-mapping-aided (3DMA) GNSS, a range of different techniques that use 3D mapping data to improve GNSS positioning accuracy in dense urban areas. The simplest form of 3DMA GNSS is terrain height aiding. For most land applications, the antenna is at a known height above the terrain. By using a digital terrain model (DTM), also known as a digital elevation model (DEM), the position solution may be constrained to a surface. In conventional least-squares positioning, this is done by generating a virtual ranging measurement [7]. By effectively removing a dimension from the position solution, this improves the accuracy of the remaining dimensions. <DELETED>

3D models of the buildings can be used to predict which signals are blocked and which are directly visible at any location [9][10]. This can be computationally intensive. However, the real-time computational load can be reduced dramatically by using building boundaries [11]. These describe the minimum elevation above which satellite signals can be received at a series of azimuths and are precomputed for each candidate position. A signal can then be classified as LOS or NLOS simply by comparing the satellite elevation with that of the building boundary at the corresponding azimuth.

The shadow-matching technique [12] determines position by comparing the measured signal availability and strength with predictions made using a 3D city model over a range of candidate positions. Several research groups have demonstrated this experimentally, using both single and multiple epochs of GNSS data [13][14][15][16][17] [18][19][20]. Cross-street position accuracies of a few meters have been achieved in dense urban areas, enabling users to determine which side of the street they're on. This complements GNSS ranging, which is more accurate in the along-street direction in these environments because more direct LOS signals are received along the street than across it. Shadow matching has also been demonstrated in real time on an Android smartphone [21]. A review of shadow matching, including its error sources and how it could be developed further may be found in [22].

3D models of the buildings can also be used to aid conventional ranging-based GNSS positioning. Where the user position is already approximately known, it is straightforward to use a 3D city model to predict the NLOS signals and eliminate them from the position solution [23][24][25]. However, for most urban positioning applications there is significant position uncertainty. <DELETED> More sophisticated approaches which score position hypotheses using the GNSS pseudo-range measurements and satellite visibility predictions at each candidate position are presented in [26] and in Section 2.2 of this paper.

Several groups have extended 3D-mapping-aided GNSS ranging by using the 3D city model to predict the path delay of the NLOS signals across an array of candidate positions [27][28][29][30]. A single-epoch positioning accuracy of 4m has been reported [29]. However, unless the search area is small, this approach is very computationally intensive as the path delay cannot easily be pre-computed. The urban

trench approach presented in [31] enables the path delays of NLOS signals to be computed very efficiently, but only if the building layout is highly symmetric, so it can only be used in suitable environments. Therefore, NLOS path delay predictions are not used in the work presented here.

3DMA GNSS ranging has also been combined with 'direct positioning' which uses the receiver correlator outputs to score an array of position hypothesis [32].

Clearly, to get the best performance out of GNSS aided by 3D mapping, as much information as possible should be used. Thus, both pseudo-range and SNR measurements from a multi-constellation GNSS receiver should be used, together with both LOS/NLOS predictions and terrain height from 3D mapping. This concept is known as intelligent urban positioning (IUP) [33].

<DELETED>

An alternative implementation of the intelligent urban positioning concept is presented in [26]. The shadow-matching algorithm is simpler than that used here. A different likelihood-based 3DMA GNSS ranging algorithm is also implemented which uses only the signals predicted to be direct LOS at each candidate position. The experimental tests demonstrate that the method works well. However, as the results presented combine measurements from multiple epochs, they are not directly comparable with the single-epoch results presented here.

Extending the IUP implementation presented here to multiple epochs for navigation and tracking applications is a subject for future work. Better performance can be expected as several researchers have already demonstrated that filtering can improve 3DMA GNSS performance [19][20][26]. Conventional GNSS positioning also works much better with multiple epochs of data. With an extended Kalman filter (within which carrier-smoothing is normally inherent), it is much easier to detect outliers due to NLOS reception and severe multipath interference than it is using single-epoch least-squares positioning. However, 3DMA GNSS also has an important role to play in multi-epoch positioning as it will enable carrier-smoothed, inertially aided and potentially even real-time kinematic (RTK) carrier-phase positioning to be accurately initialized and re-initialized in challenging urban environments.

The IUP algorithms are designed for outdoor positioning in dense urban areas. They do not work indoors and are not needed in open areas where conventional GNSS positioning works well. To determine when to use IUP, it is thus necessary to detect the environmental context. Indoor-outdoor context detection has been demonstrated using both GNSS [35][36][37][38] and Wi-Fi [37][38][39]. However, GNSS-based approaches were found to be more reliable. Therefore, here GNSS-based indoor-outdoor context detection is developed further here. A full implementation of context-adaptive navigation should also consider behavioural context and its association with environmental context [2] [37][38].

Sections 2 and 3 are DELETED. Section 4 then discusses the practicality of real-time implementation of intelligent urban positioning. Section 5 describes environmental context detection using GNSS signals. Finally, Sections 6 and 7 summarize the conclusions and plans for future work, respectively.

2. 3DMA GNSS POSITIONING ALGORITHMS

<DELETED>

3. 3DMA GNSS EXPERIMENTAL RESULTS

<DELETED>

4. PRACTICAL IMPLEMENTATION OF 3DMA GNSS

There are four ways in which 3D-mapping-aided GNSS, including the intelligent urban positioning algorithms presented here, could be implemented in a practical system:

- Post-processing of recorded data is suited to data collection applications such as mapping, and monitoring the movement of people, animals or vehicles for research purposes.
- Real-time implementation on a remote server is suited to location-based services requiring a one-time position fix and to tracking applications with long update intervals.
- Real-time implementation on a mobile device using pre-loaded mapping data is suited to professional navigation and continuous tracking applications within a limited area.
- Real-time implementation on a mobile device using streamed mapping data is suited to consumer and professional navigation and continuous tracking applications.

A practical real-time implementation of any 3DMA GNSS system requires the following [41]:

- Real-time access to GNSS pseudo-range and SNR or C/N_0 measurements;
- Computationally efficient positioning algorithms;
- Access to 3D mapping data;
- A means of distributing the GNSS measurements and mapping data to the positioning algorithms.

Survey receivers have always provided the necessary GNSS measurements, but are not practical for most 3DMA GNSS applications. Obtaining them from consumer receivers has historically been problematic. However, today, receivers such as the u-blox M8T provide pseudo-range and SNR measurements from all GNSS constellations and a new interface provides access to this data through the application programming interface (API)

on smartphones and tablets running the Android Nougat operating system that have a compatible GNSS chipset.

By using building boundaries instead of accessing the 3D mapping directly, the intelligent urban positioning algorithms presented here are able to run quickly. <DELETED>

CityGML (the Open Geospatial Consortium's approved standard for storage and exchange of virtual 3D city models, [42]) defines 3D city models as having varying levels of detail (LOD) [43]. LOD 0 is a digital terrain model, sometimes called a 2.5D model. LOD1 is a block model without any roof structures, i.e. all the buildings have flat roofs. Finally, LOD 2 is a full 3D city model having explicit roof structures and potentially associated texture.

City models are commonly stored using a boundary-representation approach, where each face (wall, floor, roof) of a building is described separately and a collection of faces grouped to represent the building. To minimize storage, these can be represented as polygons, described by the coordinates of each node (corner point). However, due to rounding errors this may not result in planar faces, which can cause problems for some of the techniques used to predict GNSS signal propagation, such as ray tracing. Thus, polygons are frequently triangulated, either on the fly or as a pre-processing stage, and a triangular mesh created prior to visualization or further processing. The greater the level of detail, the greater the number of triangles and hence the greater the time required for triangulation and the computational complexity of subsequent steps. Figures 12 and 13 show two 3D models of the same area of London, with Figure 12 derived from LOD 1 data and Figure 13 derived from LOD 2 data.

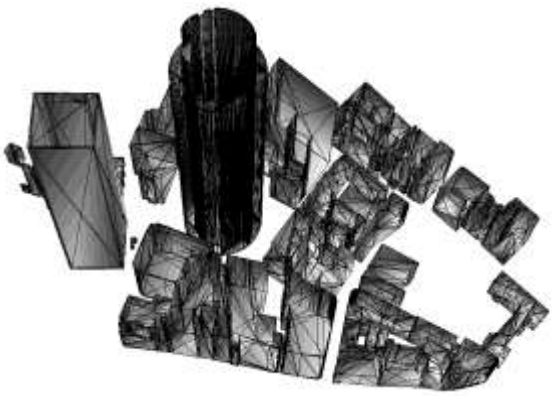

Figure 12. LOD 1 3D model of Central London near Fenchurch Street (data from Ordnance Survey)

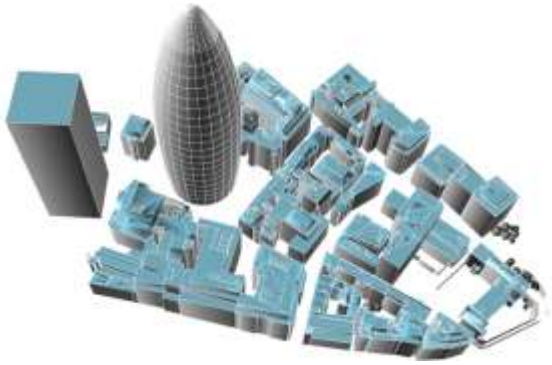

Figure 13. LOD 2 3D model of Central London near Fenchurch Street (data from Z Mapping)

Highly detailed 3D mapping is expensive. However, LOD 1 models are sufficient for most 3D-mapping-aided GNSS implementations. Open Street Map provides freely available building mapping for the world's major cities and many other places, much of it in 3D. Data is also available from national mapping agencies. Although coverage is not universal, it tends to be available in the dense urban areas where it is most needed.

This leaves data distribution. For server-based positioning, existing assisted GNSS interfaces can be used to transmit pseudo-range and SNR measurements from mobile devices to a server.

To run the positioning algorithms on a mobile device, mapping data is required. The terrain height data are easiest to handle. A 5m grid spacing is sufficient, corresponding to 40,000 points per km^2. 12 bits is sufficient to describe the relative height of a point within a tile, while 4 bytes are needed for the height of each tile's origin with respect to the datum. Thus, about 60 kB per km^2 is needed, so 1GB of storage could accommodate about 17,000 km^2 of data, much more with compression. Thus, this data could be pre-loaded in a mobile device.

Building boundaries require a lot more data. To a 1° precision, about 300 bytes are needed per building boundary. Assuming about half the space in a city is outdoor (building boundaries are not required for indoor locations), a 100×100m tile would require 1.5MB of data without compression, so 1GB of storage would only accommodate about 7 km^2 of data, maybe 70 km^2 with compression. Thus, pre-loading is only practical for users that operate within a relatively small area.

To stream building boundary data, only the search area is needed, which should be no bigger than 100×100m, considering only outdoor locations. Furthermore, only azimuths corresponding to the current set of GNSS satellites are needed, which reduces the amount of data required to 90kB without compression. Less than a kilobyte of terrain height data would be needed. 3G mobile download speeds are higher than 500 kB/s (4 Mbit/s). Therefore, streaming is easily practical and substantial data buffering could be accommodated to bridge gaps in

communications coverage. Note that for continuous positioning, successive search areas will considerably overlap so it is not necessary to transmit a full set of mapping data at every epoch.

5. ENVIRONMENTAL CONTEXT DETECTION

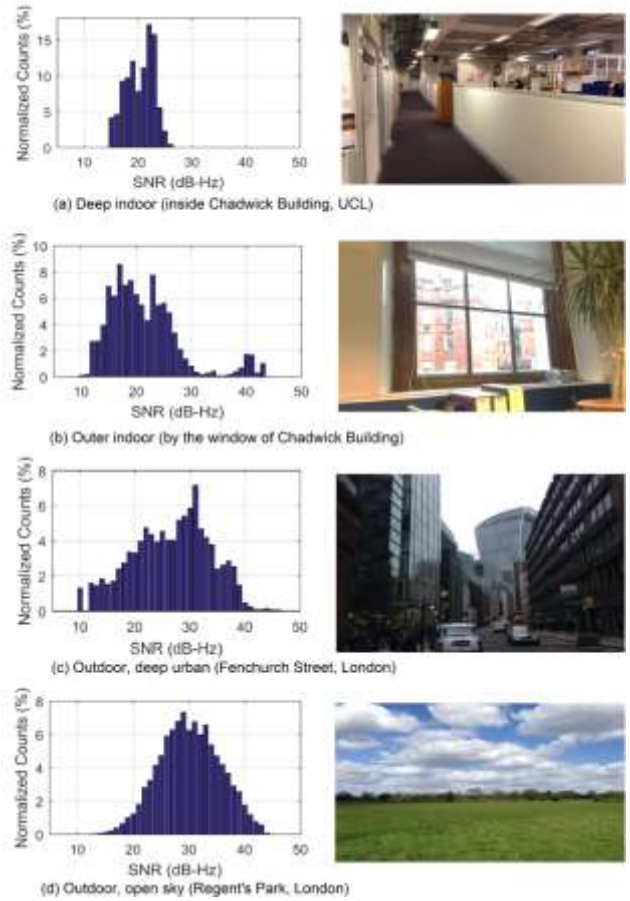

Figure 14. SNR measurement distributions under different environments

To develop a GNSS-based environmental context determination algorithm, GNSS measurements were collected at 1 Hz from both GPS and GLONASS signals received by the smartphone. The data was collected at different locations of various indoor and outdoor environments, such as deep indoor, urban, outer indoor and open sky. About 200s of static data was collected at each site. Figure 14 presents histograms showing the normalised distributions of signal-to-noise ratio (SNR) measurements from four types of environment.

A number of trends may be identified from the histograms. A signal with a higher SNR is more likely to be LOS (Line-of-Sight) than NLOS (Non-Line-of-Sight). As expected, the average received SNR is lower in indoor environments than in deep urban and open sky environments, which is useful for environmental context detection. By comparing the GNSS SNR distributions, it can also be seen that the proportions of signals weaker than 25 dB-Hz vary between different environment types. Almost all the signals received in deep indoor environments are weaker than 25 dB-Hz while increasing proportions of signals stronger than 25 dB-Hz are observed for outer indoor, deep urban and open sky.

The number of satellites received and the total measured SNR, summed across all the satellites received at each epoch, were considered as features for the environmental classification algorithm. However, these were found to be poor at distinguishing the outer indoor and deep urban environments [2].

As a larger percentage of weak signals (less than 25 dB-Hz) are received indoors than outdoors, it was found that the differences in the classification features between environments are greater if these signals are deducted from the observations. Therefore context detection here is based on two features:

- The total number of GNSS signals received with an SNR of 25 dB-Hz or more, numSNR25;
- The sum of the SNRs of the GNSS signals received with an SNR of 25 dB-Hz or more, sumSNR25.

These features are plotted in Figure 15 for the test environments shown in Figure 14, demonstrating that all four environments can be distinguished using these features.

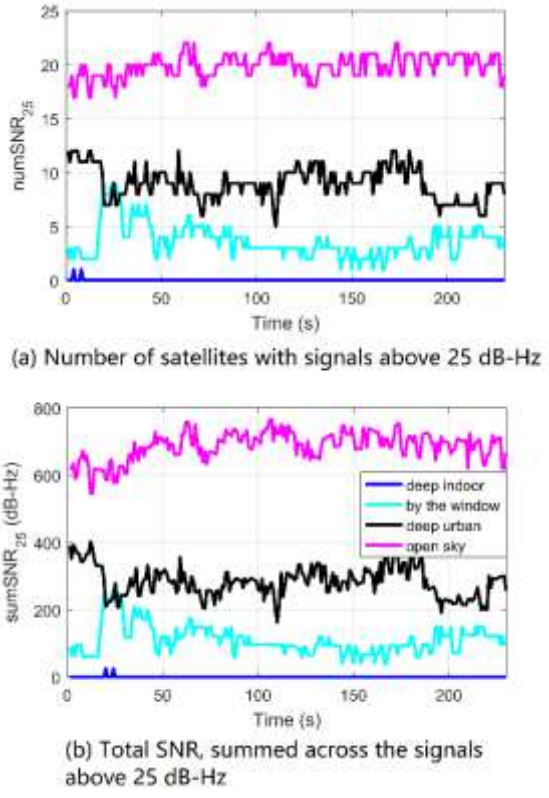

Figure 15. Features based on signals above 25 dB-Hz

In reality, the boundaries between indoor and outdoor environment can be ambiguous, rendering some scenarios hard to classify as either one. For a practical detection system, an uncertain decision is better than a wrong classification. Because an uncertain environment decision

can be used in other ways (e.g. environment connectivity, environment and behaviour association) to improve the classification, but a wrong classification cannot. Similarly, it is better to inform a context-adaptive navigation system that the environment is uncertain than to provide it with an incorrect context. Therefore, to have a smooth transition between indoor and outdoor categories and reduce the likelihood of wrong classification, a new environment category of "intermediate" is introduced to serve as a bridge between the indoor and outdoor categories. The portico of UCL's Wilkins building, shown in Figure 16, is a typical example of an intermediate environment. This is covered by the roof of the building, but there is only one wall and the other three sides of this area are open.

Figure 16. The portico of UCL's Wilkins building, an example of the intermediate category

The features $numSNR_{25}$ and $sumSNR_{25}$ can be computed sequentially from the outputs of a GNSS receiver module. A hidden Markov model (HMM) is used in this study to determine the environmental context by integrating the observations over time.

The HMM assumes a Markov process with the states that cannot be visible directly [44] (indoor, intermediate or outdoor environment in this study), so that it is capable of modelling the inherent dynamic temporal relationships of environments. In general, a HMM comprises the following five elements [2]:

1) The state space **S** that consists of N hidden states $\mathbf{S}=\{S_1, S_2,\ldots, S_N\}$. In this research, there are only three hidden states: indoor, intermediate and outdoor, which are denoted as S_1, S_2 and S_3 respectively. At each epoch k, the probabilities that the system is in each state sum to unity.

2) The set of observations at each epoch k, $Z_k= \{z_{1,k}, z_{2,k},\ldots, z_{\ell,k},\ldots, z_{m,k}\}$, where $z_{\ell,k}$ is the ℓ-th observation at epoch k and m is the number of observations. In this study, $z_{1,k}$ refers to $numSNR_{25}$ while $z_{2,k}$ is $sumSNR_{25}$.

3) The matrix of state transition probabilities $\mathbf{A}=\{A_{ij}\}$. Each element of the state transition probabilities matrix, A_{ij}, defines the probability that the state transits from a value S_i at the immediately prior epoch to another value S_j at the current epoch. The following values are assumed:

k / k+1	Indoor	Intermediate	Outdoor
Indoor	2/3	1/3	0
Intermediate	1/3	1/3	1/3
Outdoor	0	1/3	2/3

4) The vector of emission probabilities $B=\{B_i(k)\}$ that defines the conditional distributions $P(Z_k|S_i)$ of the observations from a specific state. The following values are assumed where $N(\mu, \sigma^2)$ denotes a normal distribution with mean μ and variance σ^2.

$$P(z_{1,k} \mid X_k = S_1) \sim N(4,1.6)$$
$$P(z_{1,k} \mid X_k = S_2) \sim N(7.5,1.36)$$
$$P(z_{1,k} \mid X_k = S_3) \sim N(9,4)$$

$$P(z_{2,k} \mid X_k = S_1) \sim N(50,2500)$$
$$P(z_{2,k} \mid X_k = S_2) \sim N(150,625)$$
$$P(z_{2,k} \mid X_k = S_3) \sim N(350,5000)$$

5) An initial state probability distribution $\Pi=\{\Pi_i\}$ that defines the probability of being state S_i at the first epoch. The following values are assumed:

$$P(X_1 = S_1) = P(X_1 = S_3) = 0.25$$
$$P(X_1 = S_2) = 0.5$$

In this paper, we use the first-order HMM, which assumes the current environmental context is only affected by the immediate previous context. This is illustrated by Figure 17. Given the sequence of the observations, the most likely sequence of hidden states can be inferred using the Viterbi algorithm [44][45]. The probabilities of the model are determined as follows.

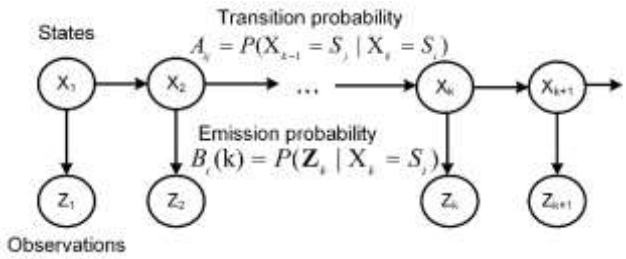

Figure 17. Structure of a first-order HMM

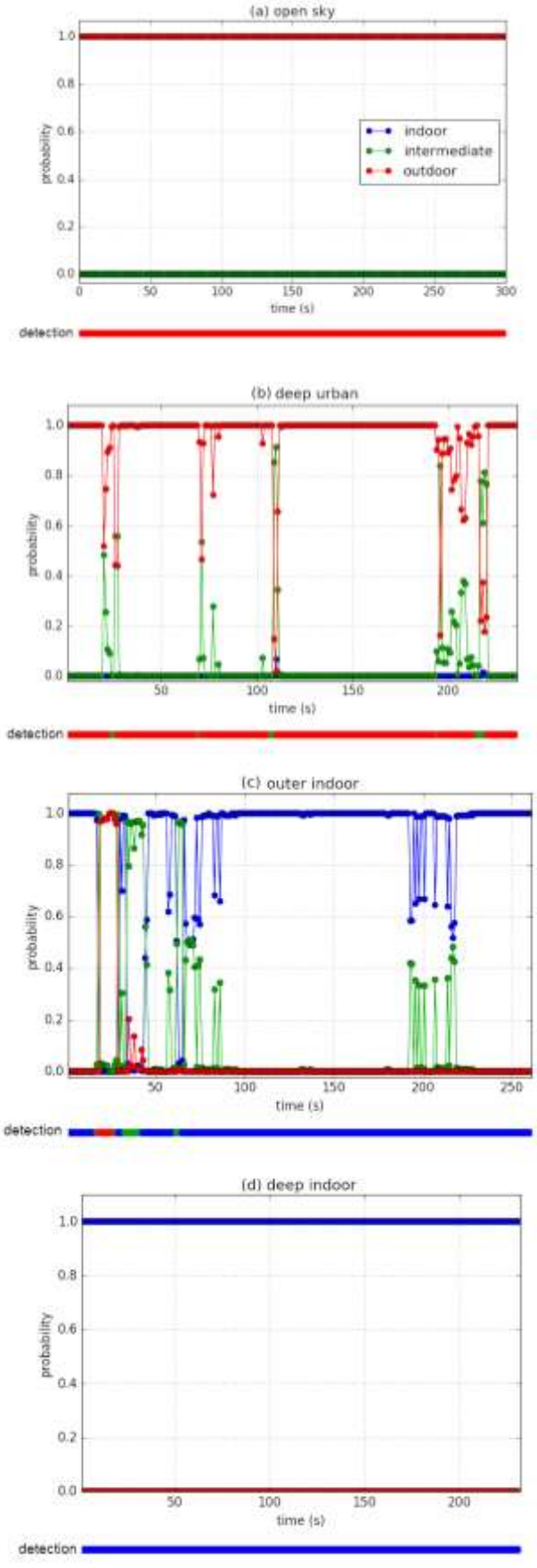

Figure 18. Static experiment results of the environment detection algorithm

Four different kinds of environment types were chosen to test the detection ability of the proposed detection method under different GNSS reception conditions. The data for open sky (outdoor), deep urban (outdoor), outer indoor and deep indoor environments are as depicted in Figure 14. Figure 18 presents the detection results of the static experiments in different environments. In the case of open sky and deep indoor, the detection results are very accurate as all samples of these scenarios are successfully detected with almost 100% probability. Deep urban is a little challenging for the detector as more signals are blocked or reflected by the tall buildings around. It can be observed from the figure that most samples are classified to outdoor correctly but with some intermediate states occasionally appearing among them. A similar thing happens for the outer indoor environment by a window. As some direct signals can still be received by the window, the measurements between 20s and 30s are erroneously classified as an outdoor environment.

6. CONCLUSIONS

<DELETED>

Finally, it has been shown that GNSS signals can be used to distinguish between indoor and outdoor environments.

6. FUTURE WORK

The following work is planned for the next year:

- <DELETED>
- Extend the GNSS-based environmental context determination algorithms to distinguish between different classes of outdoor environment in order to determine when the receiver is in an environment where it can benefit from intelligent urban positioning.

Longer term aspirations include:

- <DELETED>
- Development of a full context-adaptive navigation system using both environmental and behavioural context.

ACKNOWLEDGEMENTS

<DELETED>

The work on context determination is funded by the UCL Engineering Faculty Scholarship Scheme and the Chinese Scholarship Council. The authors would like to thank Dr. Mark Herbster and Dr. Simon Julier of UCL's Department of Computer Science for their useful comments and suggestions.

REFERENCES

[1] <RETRACTED>

[2] Gao, H. and Groves, P. D., "Context Determination for Adaptive Navigation using Multiple Sensors on a Smartphone," Portland, Oregon. Also available from http://discovery.ucl.ac.uk/.

[3] Groves, P. D., "GNSS Solutions: Multipath vs. NLOS signals. How Does Non-Line-of-Sight Reception Differ From Multipath Interference," *Inside GNSS Magazine*, Nov/Dec 2013, pp. 40-42, 63.

[4] Groves, P. D., *Principles of GNSS, inertial, and multi-sensor integrated navigation systems*, Second Edition, Artech House, 2013.

[5] Bhuiyan M. Z. H. and Lohan, E. S., "Multipath Mitigation Techniques for Satellite-Based Positioning Applications," in Jin, S. (Ed.) *Global Navigation Satellite Systems: Signal, Theory and Applications*, InTech, 2012, pp. 405-426

[6] Groves, P. D. and Jiang, Z., "Height Aiding, C/N0 Weighting and Consistency Checking for GNSS NLOS and Multipath Mitigation in Urban Areas". *Journal of Navigation*, 66, 2013, 653–669. Also available from http://discovery.ucl.ac.uk/.

[7] Amt, J. R. and Raquet, J. F., "Positioning for Range-Based Land Navigation Systems Using Surface Topography," *Proc. ION GNSS* 2006, Fort Worth, TX, 1494–1505.

[8] <RETRACTED>

[9] Bradbury, J., Ziebart, M., Cross, P. A., Boulton, P. & Read, A., "Code Multipath Modelling in the Urban Environment Using Large Virtual Reality City Models: Determining the Local Environment". *Journal of Navigation,* 60(1), 2007, 95-105.

[10] Suh, Y. and Shibasaki, R.., "Evaluation of satellite-based navigation services in complex urban environments using a three-dimensional GIS". *IEICE Transactions on Communications,* E90-B**,** 2007, 1816-1825.

[11] Wang, L., Groves, P. D. and Ziebart, M. K., "Multi-Constellation GNSS Performance Evaluation for Urban Canyons Using Large Virtual Reality City Models," *Journal of Navigation*, 65(3), 2012, 459–476. Also available from http://discovery.ucl.ac.uk/.

[12] Groves, P. D., "Shadow Matching: A New GNSS Positioning Technique for Urban Canyons". *Journal of Navigation*, 64(3), 2011, 417-430. Also available from http://discovery.ucl.ac.uk/.

[13] Ben-Moshe, B., et al., "Improving Accuracy of GNSS Devices in Urban Canyons". *23rd Canadian Conference on Computational Geometry*, 2011.

[14] Wang, L., Groves, P. D. and Ziebart, M. K., "GNSS Shadow Matching Using A 3D Model of London". *European Navigation Conference*, London, 2011. Also available from http://discovery.ucl.ac.uk/.

[15] Suzuki, T., and Kubo, N., "GNSS Positioning with Multipath Simulation using 3D Surface Model in Urban Canyon". *ION GNSS* 2012, Nashville, TN.

[16] Wang, L., Groves, P. D. and Ziebart, M. K., "GNSS Shadow Matching: Improving Urban Positioning Accuracy Using a 3D City Model with Optimized Visibility Prediction Scoring". *NAVIGATION*, 60(3), 2013, 195–207. (First published at *ION GNSS,* 2012, Nashville, TN). Also available from http://discovery.ucl.ac.uk/.

[17] Isaacs, J. T., Irish, A. T., et al., "Bayesian localization and mapping using GNSS SNR measurements". *IEEE/ION PLANS* 2014. Monterey, California.

[18] Wang, L., Groves, P. D. and Ziebart, M. K., "Smartphone Shadow Matching for Better Cross-street GNSS Positioning in Urban Environments". *Journal of Navigation*, 68(3), 2015, 411–433. Also available from http://discovery.ucl.ac.uk/.

[19] Wang, L., *Investigation of Shadow Matching for GNSS Positioning in Urban Canyons*, PhD Thesis, University College London, 2015. Available from http://discovery.ucl.ac.uk/.

[20] Yozevitch, R. and Ben-Moshe, B., "A Robust Shadow Matching Algorithm for GNSS Positioning," *NAVIGATION*, 62(2), 2015, 95–109.

[21] Wang, L., Groves, P. D. and Ziebart, M. K., "Urban Positioning on a Smartphone: Real-time Shadow Matching Using GNSS and 3D City Models". *ION GNSS*+ 2013, Nashville, Tennessee. AND *Inside GNSS*, Nov/Dec 2013, 44–56. Also available from http://discovery.ucl.ac.uk/.

[22] Groves, P. D., Wang, L., Adjrad, M., and Ellul, C., "GNSS Shadow Matching: The Challenges Ahead". *ION GNSS*+ 2015, Tampa, Florida. Also available from http://discovery.ucl.ac.uk/.

[23] Obst, M., S. Bauer, and G. Wanielik, "Urban Multipath Detection and mitigation with Dynamic 3D Maps for Reliable Land Vehicle Localization," *IEEE/ION PLANS* 2012.

[24] Bourdeau, A. and Sahmoudi, M., "Tight Integration of GNSS and a 3D City Model for Robust Positioning in Urban Canyons". *ION GNSS* 2012*,* Nashville, Tennessee.

[25] Peyraud, S., et al., "About Non-Line-Of-Sight Satellite Detection and Exclusion in a 3D Map-Aided Localization Algorithm," *Sensors*, Vol. 13, 2013, pp. 829-847.

[26] Suzuki, T., "Integration of GNSS Positioning and 3D Map using Particle Filter" *ION GNSS*+ 2016, Portland, Oregon.

[27] Suzuki, T., and Kubo N., "Correcting GNSS Multipath Errors Using a 3D Surface Model and Particle Filter," *ION GNSS*+ 2013, Nashville, TN.

[28] Kumar, R. and Petovello, M, G., "A Novel GNSS Positioning Technique for Improved Accuracy in

Urban Canyon Scenarios using 3D City Model", *ION GNSS*+ 2014, Tampa, FL.

[29] Hsu, L.-T., Gu, Y., and Kamijo, S., "3D building model-based pedestrian positioning method using GPS/GLOANSS/QZSS and its reliability calculation", *GPS Solutions*, 2015, doi 10.1007/s10291-015-0451-7.

[30] Kumar, R. and Petovello, M, G., "Sensitivity Analysis of 3D Building Model-assisted Snapshot Positioning", *ION GNSS*+ 2016, Portland, Oregon.

[31] Betaille, D., et al., "A New Modeling Based on Urban Trenches to Improve GNSS Positioning Quality of Service in Cities". *IEEE Intelligent Transportation Systems Magazine*, 5(3), 2013, 59–70.

[32] Ng, Y. and Gao, G. X., "Direct Positioning Utilizing Non Line of Sight (NLOS) GPS Signals", *ION GNSS*+ 2016, Portland, Oregon.

[33] Groves, P. D., Jiang, Z., Wang, L. and Ziebart, M., "Intelligent Urban Positioning using Multi-Constellation GNSS with 3D Mapping and NLOS Signal Detection". *ION GNSS* 2012. Nashville, Tennessee. Also available from http://discovery.ucl.ac.uk/.

[34] <RETRACTED>.

[35] Lin, T., C. O'Driscoll, and G. Lachapelle, "Channel Context Detection and Signal Quality Monitoring for Vector-based Tracking Loops," *Proc. ION GNSS 2010*.

[36] Lin, T., C. O'Driscoll, and G. Lachapelle, "Development of a Context-Aware Vector-Based High-Sensitivity GNSS Software Receiver," *Proc. ION ITM*, Jan. 2011.

[37] Groves, Paul D., et al. "Context detection, categorization and connectivity for advanced adaptive integrated navigation." *ION GNSS+ 2013*.

[38] Groves, Paul D., et al. "The four key challenges of advanced multisensor navigation and positioning." *IEEE/ION PLANS 2014*.

[39] Shafiee, M., K., O'Keefe, and G. Lachapelle, "Context-aware Adaptive Extended Kalman Filtering Using Wi-Fi Signals for GPS Navigation," *Proc. ION GNSS 2011*.

[40] <RETRACTED>.

[41] Groves, P. D., "It's Time for 3D-Mapping-Aided GNSS". *Inside GNSS*, Sep/Oct 2016.

[42] OGC 2015, *CityGML Standard, Open Geospatial Consortium*, http://www.opengeospatial.org/ standards/citygml [Accessed 3rd February 2015]

[43] Kolbe, T. H., Groger, G. and Plumer, L., "CityGML: Interoperable access to 3D city models." In: *Geo-information for disaster management*, Springer, 2005, 883–899.

[44] Bishop, Christopher M., *Pattern recognition and machine learning*. Company New York, 2006.

[45] Viterbi, Andrew J. "Error bounds for convolutional codes and an asymptotically optimum decoding algorithm." *Information Theory, IEEE Transactions on* 13.2 (1967): 260-269.